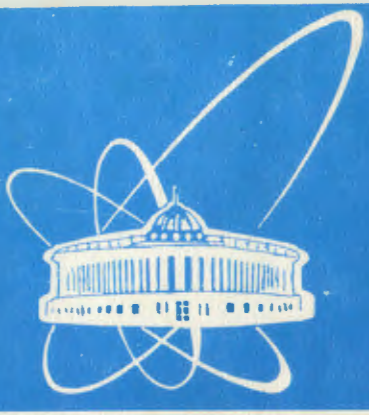

ОБЪЕДИНЕННЫЙ
ИНСТИТУТ
ЯДЕРНЫХ
ИССЛЕДОВАНИЙ

Дубна

99-156

E11-99-156

A.M.Ermolaev[1], I.V.Puzynin, A.V.Selin[2], S.I.Vinitsky

INTEGRAL BOUNDARY CONDITIONS FOR THE TIME-DEPENDENT SCHRÖDINGER EQUATION

Submitted to «Physical Review A»

[1]Physique Théorique, Faculté des Sciences, Université Libre de Bruxelles, Campus Plaine, B-1050, Bruxelles, Belgium
E-mail: ermolaev@ulb.ac.be
[2]E-mail: selin@thsun1.jinr.ru

1999

I. INTRODUCTION

Several nonperturbative methods such as Floquet [1], Sturmian-Floquet [2], and R-matrix-Floquet [3] methods, have been developed to treat the time-dependent Schroedinger equation (TDSE) for an atom interacting with the classical laser field. These methods are particularly suited moderate intensities and long laser pulses. However, experimental techniques now move towards generating super-intense and super-short laser pulses. New theoretical methods have to be developed to accommodate these experimental conditions. The numerical solution of the TDSE on a time-space grid is a recognized powerful method. This approach has been found particularly important for the adequate description of such processes as multiphoton ionization (MPI), stabilization and high-harmonics generation (HHG). The TDSE calculations on atomic hydrogen [4–6] and on atomic helium [7] have been recently reported. Despite marked success of the TDSE calculations certain limitations of the method have now become apparent.

Usually, the time-dependent quantum-mechanical problem

$$\mathrm{i}\partial_t \Psi(\mathbf{x},t) = H(t)\Psi(\mathbf{x},t) \tag{1.1}$$

is formulated as an initial value problem in an infinite domain of the configuration space $\mathbb{R}^3$ with the requirement that the wave function vanishes at an infinitely far surface,

$$|\Psi(\mathbf{x},t)| \to 0, \quad |\mathbf{x}| \to +\infty. \tag{1.2}$$

The Hamiltonian $H(t)$ in (1.1) is,

$$H(t) = \frac{1}{2}(\mathbf{p}-\mathbf{A})^2 + V(\mathbf{x}), \tag{1.3}$$

where $\mathbf{x}$ and $\mathbf{p} = -\mathrm{i}\nabla_{\mathbf{x}}$ are the position and momentum vectors of the electron, $V(\mathbf{x})$ is the atomic potential and $\mathbf{A}$ is the vector-potential. In the dipole approximation which will be considered in this paper, $\mathbf{A}$ is a function of time t only. The electric field $\mathcal{E}(t)$ corresponding to $\mathbf{A}$ is given by $\mathcal{E}(t) = -\partial_t \mathbf{A}(t)$.

In numerical applications, the zero-value boundary condition is usually replaced by one imposed at a finite distance from the atom. Once the space-domain is chosen to be finite, retaining some rigid boundary conditions causes unphysical reflection of the wave packet at the boundary and the reflected part of the packet is fed back into the system. Various techniques have been developed in order to compensate the effect. The correction is achieved by either introducing an absorbing component into the potential [8], using mask functions [9], or introducing complex coordinate contours [10]. However, by its nature, these corrections have to be made at a large distance from the atom and they are approximate. Moreover, the domain of the configuration space where the solution has to be accurately obtained, may be large for ionization rate problems and even larger for treating MPI [11]. Therefore, though absorbing boundaries and mask-functions work as a practical prescription, they do not relieve the numerical integration methods from the necessity of using over-extended space-grids.

A possible way of resolving these difficulties is to re-formulate the problem and impose some conditions on an intermediate surface. For time-independent quantum problems, there is known a variety of theoretical methods such, for instance, as the R-matrix

method [12] and the finite-range method [13], where either partial or full scattering problem is formulated within a finite domain of $\mathbb{R}^3$. We also note an extension of the R-matrix method to time-dependent problems [14]. The present work also uses a partition of the configuration space though in a context different from one of the above methods.

In a recent paper, Boucke *et al.* [15] have suggested a particular way of imposing integral boundary conditions (IBC). They applied the IBC to a one-dimensional atom with a short-range potential in a strong laser field, within the electric-dipole approximation. Their results demonstrate a certain advantage of the method for calculating ionization probability and energy spectrum. Their treatment, however, assumes the field-free asymptotic motion of the electron which is not a very accurate assumption, particularly for strong fields and long-range potentials. Also, as a consequence of their approach, it was necessary to carry out all calculations in the Kramers-Henneberger frame [16] where the interaction is localized.

In the present paper, we consider a more general IBC approach based on a theory of the parabolic potentials of the simple and double layers. We note that the reduction of the original differential equations to an integral form using the Green's functions, is a method which has been known in mathematical physics for a long time. Though it had been applied before to elliptic, hyperbolic and parabolic equations [17], apparently, it has not been used yet for the time-dependent Schrödinger equation. In our formulation, we use the integral form of the equation to impose a constraint on the solution of the initial value problem. The choice of the surface where the constraint has to be applied should be made such that it would assure the correct asymptotic behavior of the TDSE solution. In principle, the proposed method is free from some restrictions imposed in [15]. Moreover, it can also be used for the general quasi-classical construction of the asymptotic Green's-functions [18,19]. As an example, a construction of the Green's function in the Coulombic case is considered within the frame of the eikonal approximation. The efficiency of the method is demonstrated by numerical calculations on a model one-dimensional atom with a short-range potential subjected to a pulsed laser field, similar to one discussed in [15].

The layout of the paper is as follows. In Section II, the derivation of the boundary conditions with help the integral equation for a Green's function is carried out for the general three-dimensional case. The cases of a spherical boundary and the Coulombic case are considered separately. In Section III, we consider the 1D case and formulate some relations needed for calculating the final spectral densities for the electron via the solution obtained in a finite region of space. In Section IV, a numerical (Crank-Nicolson-Galerkin) method is formulated which uses a finite difference representation of the integral boundary conditions. In Section V, we apply our IBC theory to the solution of a model-1D TDSE and discuss the results, in comparison with the CC, the rigid boundary, and the Boucke et al [15] methods. Section VI concludes the paper.

II. BOUNDARY CONDITIONS

A. Parabolic potentials

We are considering the general case of a three-dimensional space $\mathbb{R}^3$. Let us denote via $G(\mathbf{x},t;\mathbf{x}',t')$ the the time-dependent Green's function of the original TDSE (1.1). This function is the solution of the problem

$$L_{\mathbf{x},t}G(\mathbf{x},t;\mathbf{x}',t') = 0, \quad t > t', \quad \mathbf{x},\mathbf{x}' \in \mathbb{R}^3, \tag{2.1}$$

where $L_{\mathbf{x},t} = \mathrm{i}\partial_t - H(\mathbf{x},t)$, and the conjugated problem

$$L^*_{\mathbf{x}',t'}G(\mathbf{x},t;\mathbf{x}',t') = 0, \quad t > t', \quad \mathbf{x},\mathbf{x}' \in \mathbb{R}^3, \tag{2.2}$$

where $L^*_{\mathbf{x}',t'} = -\mathrm{i}\partial_{t'} - H^*(\mathbf{x}',t')$. The same initial condition

$$G(\mathbf{x},t;\mathbf{x}',t') \to \delta^{(3)}(\mathbf{x}-\mathbf{x}'), \quad t' \to t, t > t'. \tag{2.3}$$

is applied in both cases. Here the operator H^* is complex conjugated to Hermitian Hamiltonian H. Note that for arbitrary functions $u(\mathbf{x},t)$ and $v(\mathbf{x},t)$ the expression $u(\mathbf{x}',t')L_{\mathbf{x}',t'}v(\mathbf{x}',t') - v(\mathbf{x}',t')L^*_{\mathbf{x}',t'}u(\mathbf{x}',t')$ can be transformed into the divergence form

$$uL_{\mathbf{x}',t'}v - vL^*_{\mathbf{x}',t'}u = \mathrm{i}\partial_{t'}(uv) + \frac{1}{2}\mathrm{div}_{\mathbf{x}'}(u\mathbf{D}_{\mathbf{x}',t'}v - v\mathbf{D}^*_{\mathbf{x}',t'}u), \tag{2.4}$$

where the differential operator $\mathbf{D}_{\mathbf{x},t}$ is given by

$$\mathbf{D}_{\mathbf{x},t} \equiv \nabla_{\mathbf{x}} - \mathrm{i}\mathbf{A}(\mathbf{x},t). \tag{2.5}$$

The integration of the relation (2.4) over a domain of the space $\mathbb{R}^3$ and time gives the well-known Green's identity.

Let W be an arbitrary finite region of $\mathbb{R}^3$ bounded by a piecewise smooth surface σ, may be disconnected. The exterior to W will be denoted via $\mathbb{R}^3 \setminus W$. Let us take in eq. (2.4) the function $u(\mathbf{x}',t')$ to be the Green's function $G(\mathbf{x},t+\epsilon;\mathbf{x}',t')$, $\epsilon > 0$, and the function $v(\mathbf{x}',t')$ to be the square-integrable solution $\Psi(\mathbf{x}',t')$ of the original TDSE,

$$L_{\mathbf{x},t}\Psi(\mathbf{x},t) = 0. \tag{2.6}$$

We integrate the identity (2.4) with respect to coordinate $\mathbf{x}'$ over the domain $\mathbb{R}^3 \setminus W$ and with respect to time t' from t_0 to t. The left hand side of (2.4) is identically zero due to (2.2) and (2.6), and the right hand side can be integrated by parts. After taking the limit $\epsilon \to 0$, one finds

$$0 = \mathrm{i}\Psi(\mathbf{x},t)\chi_W(\mathbf{x}) - \mathrm{i}\int_{\mathbb{R}^3\setminus W} \mathrm{d}^3\mathbf{x}' G(\mathbf{x},t;\mathbf{x}',t_0)\Psi(\mathbf{x}',t_0) - \frac{1}{2}\int_{t_0}^{t}\mathrm{d}t'\int_{\sigma}\mathrm{d}\sigma'\{G\mathbf{D}'\Psi(\mathbf{x}'_\sigma,t') - \Psi(\mathbf{x}'_\sigma,t')\mathbf{D}^{*\prime}G\}, \tag{2.7}$$

where $d\sigma$ is a vector-element of the surface σ which is pointed outward W. Here it has been used that the wave function at large distances tends to zero sufficiently fast so that the surface integral taken over the outer surface at infinity vanishes.

The function χ_W in (3.2) is a characteristic function discontinuous in $\mathbb{R}^3$, which is defined [20] as follows*:

$$\chi_W(\mathbf{x}) \equiv \lim_{\epsilon \to 0} \int_{\mathbb{R}^3 \setminus W} \mathrm{d}^3\mathbf{x}' G(\mathbf{x}', t+\epsilon, \mathbf{x}', t) = \begin{cases} 1, & \mathbf{x} \in \mathbb{R}^3 \setminus W, \mathbf{x} \notin \sigma, \\ \frac{1}{2}, & \mathbf{x} \in \sigma, \\ 0, & \mathbf{x} \in W, \mathbf{x} \notin \sigma, \end{cases} \tag{2.8}$$

Let us denote by μ and ν the values of the wave function and its normal derivative on σ, thus

$$\Psi\Big|_\sigma = \mu(\mathbf{x}_\sigma, t), \quad \mathbf{n}_\sigma \cdot \mathbf{D}_{x,t}\Psi\Big|_\sigma = \nu(\mathbf{x}_\sigma, t), \tag{2.9}$$

where $\mathbf{n}_\sigma$ is a unit vector normal to the surface σ and directed outward W. We introduce functions v, w, and F associated with these quantities, according to

$$v(\mathbf{x}, t) = -\int_{t_0}^{t} \mathrm{d}t' \int_\sigma \mathrm{d}\sigma'\, \nu(\mathbf{x}'_\sigma, t') G(\mathbf{x}, t, \mathbf{x}'_\sigma, t'), \tag{2.10}$$

$$w(\mathbf{x}, t) = \int_{t_0}^{t} \mathrm{d}t' \int_\sigma \mathrm{d}\sigma'\, \mu(\mathbf{x}'_\sigma, t')\, \mathbf{n}'_\sigma \cdot \mathbf{D}^*_{x',t'} G(\mathbf{x}, t, \mathbf{x}'_\sigma, t'), \tag{2.11}$$

$$F(\mathbf{x}, t) = \int_{\mathbb{R}^3 \setminus W} \mathrm{d}^3\mathbf{x}'\, \Psi(\mathbf{x}', t_0) G(\mathbf{x}, t, \mathbf{x}', t_0). \tag{2.12}$$

Here the time moment t_0 is the initial time moment for the initial-value problem (1.1).

Due to the singularity of G, the quantities defined by eqs. (2.10-2.12) can be considered as potentials generated by some surface and volume mass distributions. Similar potentials appear in the general theory of parabolic equations [20]. In the present case of the Schrödinger equation, we shall use the same terminology as in [20] and refer to (2.10-2.12) as to parabolic potentials. Then v is a simple-layer parabolic potential with the surface density ν, w is a double-layer parabolic potential with the surface density μ, and F is the initial-value parabolic potential. Making use of these quantities, equation (2.7) can be re-written as follows:

$$\Psi(\mathbf{x}, t)\chi_W = F(\mathbf{x}, t) + \frac{\mathrm{i}}{2}\{v(\mathbf{x}, t) + w(\mathbf{x}, t)\}, \quad \mathbf{x} \in \mathbb{R}^3, \tag{2.13}$$

for any $t > t_0$. This formula is a general relation satisfied by the solution of eq. (1.1) for an arbitrarily region W enclosed by a surface σ. It has a form of an integral equation which determines the wave function $\Psi(\mathbf{x}, t)$ through the parabolic potentials (2.10-2.12). As these potentials are defined in terms of the full Green's function, eq.(2.13) can be used for constructing the solution of (1.1) only within some method of successive approximations.

---

*The convergence of the integral is assured by endowing the time variable t with an infinitesimal imaginary part which has the proper sign, $t \to te^{-\mathrm{i}0}$

B. Integral boundary conditions

Now we shall discuss an application of (2.13) which is important in the numerical solution of (1.1). Let us consider the special case where the point $\mathbf{x}$ is on the surface σ. Then the equation (2.13) takes the form:

$$\mu(\mathbf{x}_\sigma, t) = 2F(\mathbf{x}_\sigma, t) + \mathrm{i}\{v(\mathbf{x}_\sigma, t) + w(\mathbf{x}_\sigma, t)\}, \tag{2.14}$$

This relation expresses the fact that values of the wave function μ and its normal derivatives ν on the surface σ cannot to be an arbitrary functions but must to satisfy the integral constraint (2.14).

The latter can be also obtained by considering the limiting passage in the eq. (2.13) as $\mathbf{x} \to \mathbf{x}_\sigma$, $\mathbf{x} \notin \sigma$. Then the continuity of the simple-layer potential and the discontinuity of the double-layer potential in the limit should be taken into account. For the potential w we have thus:

$$\lim_{\mathbf{x} \to \mathbf{x}_\sigma} w(\mathbf{x}, t) = \mp \mathrm{i}\mu(\mathbf{x}_\sigma, t) + w(\mathbf{x}_\sigma, t), \tag{2.15}$$

where the upper sign $(-)$ corresponds to approaching the surface from outside and the lower sign $(+)$ corresponds to approaching it from inside the internal region W. Due to the continuity of the wave function, the limits of the (2.13) from inside and outside of the surface σ give, of course, the same result (2.14).

The numerical solution of the TDSE proceeds, ideally, within the full configuration space $\mathbb{R}^3$. If we partition it, in an arbitrary manner, into two parts (interior, which contains the atomic nucleus, and exterior) separated by a surface σ, it would be impossible to impose the exact zero-value conditions on Ψ on such σ. However, eq. (2.14) represents a continuity condition which the solution satisfies on this surface and as such it can be used to formulate the integral boundary condition for a suitable surface.

Let us consider a surface σ which is sufficiently remote from the atom. Then an asymptotic form G_{as} can be used instead of the full Green's function $G(\mathbf{x}, t; \mathbf{x}', t')$ as will be shown below. The choice of σ and the asymptotic form depends on the properties of the atomic potential $V(\mathbf{x})$.

First, we shall consider the case of a short-range potential V and choose the domain W large enough for V to be neglected outside it. Then in the outside region the motion of the particle can be described by an asymptotic Hamiltonian $H_{as}(t)$,

$$H_{as}(t) = \frac{1}{2}\Big(-\mathrm{i}\nabla_{\mathbf{x}'} - \mathbf{A}(t)\Big)^2. \tag{2.16}$$

The explicit form of the Green's function G_{as} of the TDSE with the Hamiltonian (2.16) is

$$G_{as}(\mathbf{x}, t; \mathbf{x}', t') = \frac{e^{\mathrm{i}S(\mathbf{x},t;\mathbf{x}',t')}}{[2\pi\mathrm{i}(t-t')]^{3/2}}, \quad t > t', \tag{2.17}$$

where S is the classical action for a particle in the field $\mathbf{A}(t)$ taken to be a function of the initial and the final position and time (the Hamilton principle function), that is

$$S(\mathbf{x}, t; \mathbf{x}', t') = \frac{[\mathbf{x} - \boldsymbol{\xi}(t) - \mathbf{x}' + \boldsymbol{\xi}(t')]^2}{2(t-t')} - \frac{1}{2}\int_{t'}^{t} \mathbf{A}^2(\tau)\mathrm{d}\tau, \tag{2.18}$$

and $\boldsymbol{\xi}(t)$ is the classical displacement of the electron due to the field given by

$$\boldsymbol{\xi}(t) = -\int_0^t \mathbf{A}(\tau)\mathrm{d}\tau \tag{2.19}$$

The form (2.17) of the G_{as} is determined by the WKB-approximation which gives the exact result for the TDSE with the Hamiltonian (2.16) (see e.g. [21]). This Green's function can also be easily obtained via an expansion in terms of the corresponding Volkov states $\Theta_{\mathbf{k}}(\mathbf{x}, t)$,

$$\Theta_{\mathbf{k}}(\mathbf{x}, t) = \mathrm{e}^{\mathrm{i}\mathbf{k}\mathbf{x} - \frac{\mathrm{i}}{2}\int_0^t (\mathbf{k}-\mathbf{A})^2 \mathrm{d}\tau}. \tag{2.20}$$

Then

$$G_{as}(\mathbf{x}, t, \mathbf{x}', t') = \int \frac{\mathrm{d}^3\mathbf{k}}{(2\pi)^3} \Theta_{\mathbf{k}}(\mathbf{x}, t)\Theta^*_{\mathbf{k}}(\mathbf{x}', t'). \tag{2.21}$$

Making use of the asymptotic Green's function G_{as}, the integral equation for the full Green's function G can be written as follows,

$$G(\mathbf{x}, t, \mathbf{x}', t') = G_{as}(\mathbf{x}, t, \mathbf{x}', t') - \mathrm{i}\int_{t'}^t \mathrm{d}t'' \int \mathrm{d}^3\mathbf{x}'' G_{as}(\mathbf{x}, t, \mathbf{x}'', t'')V(\mathbf{x}'', t'')G(\mathbf{x}'', t'', \mathbf{x}', t'), \tag{2.22}$$

where integration over $\mathbf{x}''$ extended to all configuration space $\mathbb{R}^3$. Multiplying both sides of this equation by density $\nu(\mathbf{x}', t')$ and integrating with respect to time t' from t_0 up to t and keeping the surface σ fixed, one finds that the simple-layer potential v satisfies the integral equation

$$v(\mathbf{x}, t) = v_{as}(\mathbf{x}, t) - \mathrm{i}\int_{t_0}^t \mathrm{d}t'' \int \mathrm{d}^3\mathbf{x}'' G_{as}(\mathbf{x}, t, \mathbf{x}'', t'')V(\mathbf{x}'', t'')v(\mathbf{x}'', t''), \tag{2.23}$$

Here the zero-order term v_{as} is a simple-layer parabolic potential constructed as in (2.10) but with the help of the asymptotic Green's function G_{as}.

$$v_{as}(\mathbf{x}, t) = -\int_{t_0}^t dt' \int_\sigma d\sigma' \nu(\mathbf{x}'_\sigma, t')G_{as}(\mathbf{x}, t, \mathbf{x}'_\sigma, t') \tag{2.24}$$

Similar integral equations can be obtained for the double-layer parabolic potentials w and w_{as} as well as for the initial-value parabolic potentials F and F_{as}.

The asymptotic form of the formula (2.13) is then obtained by substituting in it the asymptotic equations derived above. Thus:

$$\Psi(\mathbf{x}, t)\chi_W(\mathbf{x}) = F_{as}(\mathbf{x}, t) + \frac{\mathrm{i}}{2}\{v_{as}(\mathbf{x}, t) + w_{as}(\mathbf{x}, t)\} - \mathrm{i}\int_{t_0}^t \mathrm{d}t'' \int \mathrm{d}^3\mathbf{x}'' G_{as}(\mathbf{x}, t, \mathbf{x}'', t'')V(\mathbf{x}'', t'')\Psi(\mathbf{x}'', t'')\chi_W(\mathbf{x}''). \tag{2.25}$$

If the potential $V(\mathbf{x}, t)$ is a short-range potential, and the domain W contains the entire region of the action of V, then the last term in eq. (2.25) is negligibly small since due to the presence of the characteristic function χ_W (2.8) the integration goes outside of the region of the action of the interaction V. Thus, in this case the the equation on the boundary has the form (2.14) where the parabolic potentials are simply replaced by the asymptotic potentials, i.e.

$$\mu(\mathbf{x}_\sigma, t) = 2F_{as}(\mathbf{x}_\sigma, t) + \mathrm{i}\{v_{as}(\mathbf{x}_\sigma, t) + w_{as}(\mathbf{x}_\sigma, t)\}. \tag{2.26}$$

Note, this boundary condition is a linear non-local in space and time relationship between boundary and initial values of wave function. Otherwise, for the potentials decaying too slow, the eq. (2.25) may need the next iteration with respect to Ψ or some other methods of solution.

C. Spherical boundary of domain W

Now we consider a particular case where the surface σ of the domain W is a sphere of large radius $R \gg a_0$ where a_0 is an effective radius of interaction. For the sake of simplicity we assume also that the initial wave function $\Psi(\mathbf{x}, t_0)$ is negligibly small in the outer domain beyond σ. Then the term $F_{as}(\mathbf{x}, t)$ in (2.26) can be dropped. Thus, our task is to find the asymptotic expressions for the parabolic potentials v_{as} and w_{as} on the sphere of a large radius R. Let us denote $\hat{\mathbf{n}} = R^{-1}\mathbf{x}_\sigma$,

$$Q(t, t') = |R\hat{\mathbf{n}} - \boldsymbol{\xi}(t) + \boldsymbol{\xi}(t')|, \quad \hat{\omega}(t, t') = \frac{R\hat{\mathbf{n}} - \boldsymbol{\xi}(t) + \boldsymbol{\xi}(t')}{|R\hat{\mathbf{n}} - \boldsymbol{\xi}(t) + \boldsymbol{\xi}(t')|}. \tag{2.27}$$

The Green's function (2.17) in terms of these notations can be written as

$$G_{as}(R\hat{\mathbf{n}}, t; R\hat{\mathbf{n}}', t') = \frac{\mathrm{e}^{\mathrm{i}\frac{R^2+Q^2}{2(t-t')} - \frac{\mathrm{i}}{2}\int_{t'}^t \mathbf{A}^2 \mathrm{d}\tau}}{[2\pi\mathrm{i}(t-t')]^{3/2}} \mathrm{e}^{-\mathrm{i}\frac{RQ}{t-t'}\hat{\mathbf{n}}'\hat{\omega}}. \tag{2.28}$$

Using the limiting expression [22] for the generalized functions, as $\lambda \to +\infty$, we write:

$$\mathrm{e}^{\mathrm{i}\lambda\hat{\mathbf{n}}\hat{\omega}} \sim \frac{2\pi}{\mathrm{i}\lambda}\left\{\mathrm{e}^{\mathrm{i}\lambda}\delta(\hat{\mathbf{n}}, \hat{\omega}) - \mathrm{e}^{-\mathrm{i}\lambda}\delta(\hat{\mathbf{n}}, -\hat{\omega})\right\}, \tag{2.29}$$

where $\delta(\hat{\mathbf{n}}, \hat{\omega})$ is the delta-function on the unit sphere. Then one can take easy the angular integrals in (2.24). For the potential v_{as} it yields

$$v_{as}(R\hat{\mathbf{n}}, t) \simeq -\int_{t_0}^t \frac{R\,\mathrm{e}^{-\frac{\mathrm{i}}{2}\int_{t'}^t \mathbf{A}^2 \mathrm{d}\tau}\mathrm{d}t'}{Q\sqrt{2\pi\mathrm{i}(t-t')}} \left\{\mathrm{e}^{\mathrm{i}\frac{(Q-R)^2}{2(t-t')}}\nu(\hat{\omega}, t') - \mathrm{e}^{\mathrm{i}\frac{(Q+R)^2}{2(t-t')}}\nu(-\hat{\omega}, t')\right\}. \tag{2.30}$$

Here we restrict our attention to such electric fields that the classical displacement (2.19) $\boldsymbol{\xi}(t)$ is bounded for all times. It means that the function $Q(t, t')$ in the last expression takes values close to R but it is never zero, provided that R is sufficiently large. Then second term in the integral (2.30) can be neglected because it contains a rapidly oscillating

exponential at $t' \to t$. To estimate the neglected quantity, let us consider the leading term of the asymptotic expansion of the following integral

$$I(\lambda) = \int_{t_0}^{t} \mathrm{d}t'(t-t')^{-\alpha} \mathrm{e}^{\mathrm{i}\lambda(t-t')^{-1}} g(t'), \quad \alpha < 2, \tag{2.31}$$

where $\lambda \to +\infty$, and $g(t')$ is a smooth nonsingular function in the segment $[t_0, t]$. By changing variables, $\rho = (t-t')^{-1}$, this integral transforms to

$$I(\lambda) = \int_{(t-t_0)^{-1}}^{+\infty} \rho^{\alpha-2} \mathrm{d}\rho \mathrm{e}^{\mathrm{i}\lambda\rho} g(t-\rho^{-1}). \tag{2.32}$$

Integrating by parts gives the leading asymptotic term, thus:

$$I(\lambda) = -\frac{(t-t_0)^{2-\alpha}}{\mathrm{i}\lambda} \mathrm{e}^{\mathrm{i}\lambda(t-t_0)^{-1}} g(t_0) + O(\lambda^{-2}). \tag{2.33}$$

Taking $\alpha = 1/2$ and $\lambda = 2R^2$ in (2.33), one finds that the absolute value of the estimated term in (2.30) is of order

$$\frac{(t-t_0)^{3/2} \nu(-\hat{\omega}(t,t_0), t_0)}{RQ(t,t_0)}. \tag{2.34}$$

Here it should be taken into account that the values of μ and ν at the initial time t_0 are negligible small, hence the second term in (2.30) can be neglected.

The case of the potential w_{as} can be dealt with in a completely analogous manner. As a result, the the relation (2.26) has the asymptotic form

$$\mu(\hat{\mathbf{n}}, t) = \int_{t_0}^{t} \frac{R}{Q} \frac{\mathrm{e}^{\mathrm{i}\frac{(Q-R)^2}{2(t-t')} - \frac{\mathrm{i}}{2}\int_{t'}^{t} \mathbf{A}^2 \mathrm{d}\tau}}{\sqrt{2\pi\mathrm{i}(t-t')}} \mathrm{d}t' \left\{ \mu(\hat{\omega}, t') \left(\frac{Q-R}{t-t'} - \hat{\omega}\mathbf{A}(t') \right) - \mathrm{i}\nu(\hat{\omega}, t') \right\}. \tag{2.35}$$

In the particular case of $\mathbf{A} \equiv 0$, this relation was obtained in [15].

D. Coulomb potential

Now we shall consider the case of a Coulomb potential. Due to a slow rate of decay, it causes the specific phase distortion in the time-independent Coulomb Green's function at large distances, in comparison with the short-range potentials [22]. This effect should be taken into account while deriving the boundary conditions. In fact, we need to obtain at large distances an approximation to the time-dependent Coulomb Green function $G_c(\mathbf{x}, t; \mathbf{x}', t')$ which satisfies the following equation

$$\mathrm{i}\partial_t G_c = \frac{1}{2}\left(-\mathrm{i}\nabla_{\mathbf{x}} - \mathbf{A}\right)^2 G_c + \frac{\alpha}{|\mathbf{x}|} G_c, \tag{2.36}$$

together with the initial condition (2.3). As follows from the physical arguments (see, e.g. [23]), the motion of the particle is semiclassical at distances much larger than Bohr

radius. Thus, for our purposes, it should be possible to apply the WKB techniques [18]. The function G_c is sought as a product:

$$G_c = C(\mathbf{x}, t; \mathbf{x}', t') \mathrm{e}^{\mathrm{i}S(\mathbf{x},t;\mathbf{x}',t')}, \tag{2.37}$$

where C and S are arbitrary real-valued functions. Substituting (2.37) into (2.36) yields the following system:

$$\begin{cases} \partial_t C^2 + \mathrm{div}\{C^2(\nabla_{\mathbf{x}} S - \mathbf{A})\} = 0, \\ \partial_t S + \frac{1}{2}(\nabla_{\mathbf{x}} S - \mathbf{A})^2 + \frac{\alpha}{|\mathbf{x}|} = \frac{\Delta_{\mathbf{x}} C}{C}, \end{cases} \tag{2.38}$$

The first line in (2.38) is the continuity equation for the density C. The second line, with the right-hand side set to zero, is the Hamilton–Jacobi equation for the action describing the classical motion of the atomic electron. The left-hand side of this equation is identically zero if the function S is taken to be the integral of the Lagrange function calculated along the classical trajectory of particle $\mathbf{X}(\tau; \mathbf{x}, \mathbf{x}')$, with the end points $\mathbf{x}$ and $\mathbf{x}'$ for $\tau = t'$ and $\tau = t$, respectively. That is

$$S = \int_{t'}^{t} \mathrm{d}\tau \left\{ \frac{\dot{\mathbf{X}}^2(\tau) + \dot{\mathbf{X}}(\tau)\mathbf{A}(\tau)}{2} - \frac{\alpha}{|\mathbf{X}(\tau)|} \right\}. \tag{2.39}$$

We note that if the Coulomb potential is absent in (2.38) then the exact trajectory $\mathbf{X}_0(\tau)$ is

$$\mathbf{X}_0(\tau) = \frac{\mathbf{x} - \boldsymbol{\xi}(t) - \mathbf{x}' + \boldsymbol{\xi}(t')}{t-t'}(\tau - t') + \boldsymbol{\xi}(\tau) - \boldsymbol{\xi}(t') + \mathbf{x}', \tag{2.40}$$

and the action (2.39) evaluated along this trajectory is exactly the expression (2.18). Moreover, if the density function C is taken to be independent of the space variables,

$$C = [2\pi\mathrm{i}(t-t')]^{-3/2} \tag{2.41}$$

then both equations of (2.38) are identically satisfied if $\alpha = 0$. The resulting function coincides with the Green's function (2.17).

In the case of $\alpha \neq 0$, we shall introduce an approximation which is similar to the eikonal approximation for the time-independent case (see [22]). Namely, the solution of (2.38) is obtained by evaluating the action S in (2.39) along the free trajectory $\mathbf{X}_0(\tau)$ given by (2.40), i.e.

$$S \approx S_0 - Z, \tag{2.42}$$

where S_0 is the expression (2.18). In eq. (2.42), the phase distortion Z is defined as

$$Z(\mathbf{x}, t; \mathbf{x}', t') = \alpha \int_{t'}^{t} \frac{\mathrm{d}\tau}{|\mathbf{X}_0(\tau)|}, \tag{2.43}$$

and the density C is the same as above (2.41). Note that this approximation does not work if the classical trajectory $\mathbf{X}_0(\tau)$ passes through the Coulomb center because in the latter case the integral (2.43) is not defined. Below we exclude this case from consideration.

In order to estimate an error in such a model, we first note that the function Z satisfies (within the assumptions stated above) the Laplas equation

$$\Delta_{\mathbf{x}} Z = 0. \tag{2.44}$$

Thus, the continuity equation (2.38) holds exactly. Secondly, the action S, eq. (2.42), satisfies the Hamilton–Jacobi equation in (2.38) only approximately. After some manipulations one finds that the error (thus, it is relative error for the solution of eq. (2.36) in the form (2.37)), is

$$\frac{1}{2}(\nabla_{\mathbf{x}} Z)^2 \sim \alpha^2 \frac{(t-t')^2}{\rho^4}, \tag{2.45}$$

where ρ is the distance of the nearest approach, from the Coulomb center to the trajectory $\mathbf{X}_0(\tau; \mathbf{x}, \mathbf{x}')$. This estimate can be useful for choosing the grid size for the numerical integration of the TDSE if one uses the approximation to G_c considered above.

The phase distortion Z depends on the particular form of the electric field $\mathbf{A}(t)$ and it should be considered in each case separately. However, in the field-free case it is evaluated explicitly to give

$$Z^{(0)}(\mathbf{x}, t; \mathbf{x}', t') = \alpha \frac{t-t'}{|\mathbf{x}-\mathbf{x}'|} \log \frac{|\mathbf{x}||\mathbf{x}-\mathbf{x}'| + (\mathbf{x}, \mathbf{x}-\mathbf{x}')}{|\mathbf{x}'||\mathbf{x}-\mathbf{x}'| + (\mathbf{x}', \mathbf{x}-\mathbf{x}')}. \tag{2.46}$$

It is interesting to notice the formal correspondence between this expression and the asymptotic distortion term in the phase of the stationary Coulomb Green's function $G_c(\mathbf{x}, \mathbf{x}', E + \mathrm{i}0)$ [22] provided that one treats the factor $\frac{t-t'}{|\mathbf{x}-\mathbf{x}'|}$ in (2.46) as $(2E)^{-1/2}$.

Considering the field-free case for the spherical boundary of radius $R \gg 1$ in just the same way as it has been done at the Sec. II C, one finds the asymptotic form of the boundary equation (2.26) with the Coulomb corrections as follows

$$\mu(\hat{\mathbf{n}}, t) = \int_{t_0}^{t} \frac{\mathrm{e}^{-\mathrm{i}\frac{\alpha}{R}(t-t')} \mathrm{d}t'}{\sqrt{2\pi \mathrm{i}(t-t')}} \left\{ -\frac{\alpha(t-t')}{2R^2} \mu(\hat{\mathbf{n}}, t') - \mathrm{i}\nu(\hat{\mathbf{n}}, t') \right\}. \tag{2.47}$$

Here we note that the asymptotics of the G_c in the singular direction $\hat{\mathbf{n}}' = -\hat{\mathbf{n}}$ for approximation (2.47) is not required.

III. APPLICATION TO 1D PROBLEM

A. Boundary conditions

We assume that the potential $V(x)$ of a model 1D atom operates in the domain $W \in \mathbb{R}$ which is a finite interval $a_- < x < a_+$. Adjacent to it are two half-open intervals: $x < a_-$

(region I) and $x > a_+$ (region II). Let us denote the values of the function $\Psi(x,t)$ and its derivative $D_{x,t}\Psi(x,t) \equiv (\partial_x - \mathrm{i}A(t))\Psi(x,t)$ at the boundaries of the regions I and II as

$$\Psi(a_\mp, t) = \mu^{I,II}(t), \quad D_{x,t}\Psi(a_\mp, t) = \nu^{I,II}(t). \tag{3.1}$$

The Green's function G_{as} in the 1D case is

$$G_{as}(x,t;x',t') = \frac{\mathrm{e}^{\mathrm{i}S(x,t;x',t')}}{\sqrt{2\pi \mathrm{i}(t-t')}}, \quad t > t', \tag{3.2}$$

where the action S is given by (2.18). The boundary equations (2.26) are then written as follows

$$\mu^{I,II}(t) = 2F_{as}^{I,II}(a_\mp, t) + \mathrm{i}\left\{ v_{as}^{I,II}(a_\mp, t) + w_{as}^{I,II}(a_\mp, t) \right\}, \tag{3.3}$$

where the parabolic potentials are defined by

$$v_{as}^{I,II}(x,t) = \pm \int_{t_0}^{t} \frac{\nu^{I,II}(t')\mathrm{d}t'}{\sqrt{2\pi \mathrm{i}(t-t')}} \mathrm{e}^{\mathrm{i}S(x,t;a_\mp,t')}, \tag{3.4}$$

$$w_{as}^{I,II}(x,t) = \mp \mathrm{i} \int_{t_0}^{t} \frac{\mu^{I,II}(t')\mathrm{d}t'}{\sqrt{2\pi \mathrm{i}(t-t')}} \left(\frac{\partial S}{\partial x'} + \frac{e}{c} A(t') \right) \mathrm{e}^{\mathrm{i}S(x,t;a_\mp,t')}, \tag{3.5}$$

$$F_{as}^{I,II}(x,t) = \int_{I,II} \frac{\Psi(x',t_0)\mathrm{d}x'}{\sqrt{2\pi \mathrm{i}(t-t_0)}} \mathrm{e}^{\mathrm{i}S(x,t;x',t_0)}. \tag{3.6}$$

Generally, the surface σ can be chosen in an arbitrary way. It is instructive to consider a special case where $V(x)$ is a zero-range potential determined by the boundary condition at the origin

$$\nu^{II}(0,t) - \nu^{I}(0,t) = 2\varkappa\mu(0,t). \tag{3.7}$$

This condition corresponds to the potential V of the form $\varkappa\delta(x)$. In this case, the domain W consists of one point, $x = 0$, that is $W = \{0\}$. It is easy to check that the half-sum of eqs. (3.3) gives, on account of (3.7), a Volterra equation for $\Psi(0,t)$, thus:

$$\Psi(0,t) = \int_{-\infty}^{+\infty} \mathrm{d}x' G_{as}(0,t,x',t_0)\Psi(x',t_0) - \mathrm{i}\varkappa \int_{t_0}^{t} \mathrm{d}t' G_{as}(0,t,0,t')\Psi(0,t'). \tag{3.8}$$

This equation provides the complete solution $\Psi(x,t)$. Alternatively, it can be obtained directly from the original TDSE (for details see [24]).

This limiting case is a good illustration of our general conclusion: in the IBC method, the size of the region W where the numerical solution is to be found, depends only on the decaying properties of the potential V. As will be shown in the numerical example below, the suggested method of imposing boundary conditions allows the region W to be chosen sufficiently small, despite the presence of a strong electric field.

B. Evaluation of spectrum

We shall now calculate the transition amplitudes $\mathcal{A}_{qn}$ for the electron that initially are found to be in the bound state $\Psi_i = \psi_n(x)$ to final state with the determined value of the kinetic momentum $\pm q$ at the remote future, $q = +\sqrt{2E}$, via the solution of (1.1) known in the internal region. It is assumed, that the pulse of the electric field has finite duration. The corresponded vector potential $A(t)$ can be chosen zero before the field is turned on. Thus, the vector potential tends to some constant value A_- after the field is turned off. In this case, the final state should be chosen

$$\Psi^{(-)}_{1,2E} = \mathrm{e}^{\mathrm{i}A_- x}\psi^{(-)}_{1,2E}, \tag{3.9}$$

where $\psi^{(-)}_{1,2E}$ is the scattering eigenstate of the Hamiltonian (1.3), where $A \equiv 0$. Here the subscripts 1 and 2 are correspond to positive and negative direction of the momentum $\pm q$, respectively. Thus, the transition amplitude is

$$\mathcal{A}_{\pm qn} = \langle \Psi^{(-)}_{1,2E} | \Psi(t) \rangle, \tag{3.10}$$

where $\Psi(t)$ is solution of the TDSE (1.1) after the laser pulse has been turned off. The spectral distribution of ejected electron $p_n(E)$ as a function of the energy E is a sum

$$p_n(E) = \frac{1}{2\pi}\left(|\mathcal{A}_{qn}|^2 + |\mathcal{A}_{-qn}|^2\right). \tag{3.11}$$

The factor $(2\pi)^{-1}$ fixes the normalization of the functions $\psi^{(-)}_{1,2E}(x)$. Also, the probability $p_{n'n}$ of the transition to bound final state $\Psi_{n'} = \mathrm{e}^{\mathrm{i}A_- x}\psi_{n'}(x)$ is given by

$$p_{n'n} = |\langle \Psi_{n'} | \Psi(t) \rangle|^2. \tag{3.12}$$

By virtue of completeness of the basis set of functions $\Psi^{(-)}_{1,2E}(x)$ and $\Psi_n(x)$, the conservation law for the total probability has the form

$$\int_0^{+\infty} \frac{\mathrm{d}E}{\sqrt{2E}} p_n(E) + \sum_{n'} p_{n'n} = 1. \tag{3.13}$$

The amplitudes $\mathcal{A}_{\pm qn}$ are a sum of three integrals, for regions I, II, W, correspondingly:

$$\mathcal{A}_{\pm qn} = \left(\int_{-\infty}^{a_-} + \int_{a_+}^{+\infty} + \int_{a_-}^{a_+}\right) {\Psi^{(-)}_{1,2E}}^* \Psi \mathrm{d}x. \tag{3.14}$$

If the solution of the problem (1.1) is known in the internal region W, e.g. as a result of the numerical calculations with the boundary conditions (3.3), then one can evaluates the integrals for regions I and II by continuing the internal solution to these regions with the help of the relations:

$$\Psi^{I,II}(x,t) = F^{I,II}_{as}(x,t) + \frac{\mathrm{i}}{2}\left\{v^{I,II}_{as}(x,t) + w^{I,II}_{as}(x,t)\right\}, \tag{3.15}$$

and using the asymptotic form of the functions ${\psi^{(-)}_{1,2E}}^* = \psi^{(+)}_{2,1E}$. These are well-known and listed in the following table:

	$\psi^{(+)}_{1E}$	$\psi^{(+)}_{2E}$
I	$\mathrm{e}^{\mathrm{i}qx} + \alpha\mathrm{e}^{-\mathrm{i}qx}$	$\beta\mathrm{e}^{-\mathrm{i}qx}$
II	$\beta\mathrm{e}^{\mathrm{i}qx}$	$\mathrm{e}^{-\mathrm{i}qx} + \gamma\mathrm{e}^{\mathrm{i}qx}$,

where coefficients $\alpha(E)$, $\beta(E)$ and $\gamma(E)$ are the S-matrix elements for scattering on the potential V.

Let us introduce for convenience two transforms:

$$\widehat{\Psi}^I(q,t) = \int_{-\infty}^{a_-} \mathrm{d}x\, \mathrm{e}^{-\mathrm{i}k_I x}\Psi(x,t) \tag{3.16}$$

and

$$\widehat{\Psi}^{II}(q,t) = \int_{a_+}^{+\infty} \mathrm{d}x\, \mathrm{e}^{-\mathrm{i}k_{II} x}\Psi(x,t), \tag{3.17}$$

where the $k_{I,II}$ are canonical momenta that correspond to the kinetic momenta $\mp q$ after electric field is turn off,

$$k_{I,II} = \mp q + A_-. \tag{3.18}$$

Making use of (3.16-3.17) and (3.14) one finds the following expression for the amplitudes

$$\begin{pmatrix} \mathcal{A}_{-qn} \\ \mathcal{A}_{qn} \end{pmatrix} = \begin{pmatrix} \widehat{\Psi}^I(q,t) \\ \widehat{\Psi}^{II}(q,t) \end{pmatrix} + \begin{pmatrix} \alpha & \beta \\ \beta & \gamma \end{pmatrix} \begin{pmatrix} \widehat{\Psi}^I(-q,t) \\ \widehat{\Psi}^{II}(-q,t) \end{pmatrix} + \begin{pmatrix} \int_{a_-}^{a_+} {\Psi^{(-)}_{2E}}^* \Psi \mathrm{d}x \\ \int_{a_-}^{a_+} {\Psi^{(-)}_{1E}}^* \Psi \mathrm{d}x \end{pmatrix}. \tag{3.19}$$

In turn, the substitution of the solution $\Psi(x,t)$ continued by (3.15) in the expressions (3.16) and (3.17) represents $\Psi^{I,II}(q,t)$ as a sum of transformed parabolic potentials,

$$\widehat{\Psi}^{I,II}(q,t) = \frac{\mathrm{i}}{2}\widehat{v}^{I,II}_{as}(q,t) + \frac{\mathrm{i}}{2}\widehat{w}^{I,II}_{as}(q,t), \tag{3.20}$$

where

$$\widehat{v}^{I,II}(q,t) = \pm \int_{t_0}^{t} \mathrm{d}t' \nu^{I,II}(t') \widehat{G}^{I,II}_{as}(q,t;a_{\mp},t'), \tag{3.21}$$

and

$$\widehat{w}^{I,II}(q,t) = \mp \int_{t_0}^{t} \mathrm{d}t' \mu^{I,II}(t') D^{*\prime} \widehat{G}^{I,II}_{as}(q,t;a_{\mp},t'). \tag{3.22}$$

In order to simplify calculations, we assume that all bound states including the initial state $\psi_n(x)$ are negligibly small in the regions I and II so that the term $\widehat{F}^{I,II}(q,t)$ can be discarded.

The mixed Green functions $\widehat{G}^{I,II}_{as}(q,t;x',t')$ above are obtained by applying transforms (3.16-3.17) to the Green's function $G_{as}(x,t;x',t')$, with respect to its first space variable x. The evaluation of the functions $\widehat{G}^{I,II}_{as}$ gives

$$\widehat{G}^{I,II}_{as}(q,t;x',t') = \mathrm{e}^{-\mathrm{i}k_{I,II}x' - \frac{\mathrm{i}}{2}\int_{t'}^{t}(k_{I,II}-A(\tau))^2\mathrm{d}\tau}\Phi(z_{I,II}), \tag{3.23}$$

where

$$z_{I,II} = \pm k_{I,II}\sqrt{\frac{t-t'}{2}} \mp \frac{a_{\mp} - \xi(t) - x' + \xi(t')}{\sqrt{2(t-t')}}, \tag{3.24}$$

and $\Phi(z)$ is the Fresnel integral,

$$\Phi(z) = \frac{1}{\sqrt{\pi\mathrm{i}}}\int_{z}^{+\infty}\mathrm{e}^{\mathrm{i}\rho^2}\mathrm{d}\rho. \tag{3.25}$$

Thus, eqs. (3.19-3.25) give the ionization amplitudes $\mathcal{A}_{\pm qn}$ in a closed form.

Now we consider the asymptotic form of (3.19) for large times t. Making use of the asymptotics $\xi(t)$ from (2.19) for the classical displacement of the electron, one finds

$$z_{I,II} = -q\sqrt{\frac{t}{2}} + O(t^{-1/2}), \quad t \to +\infty. \tag{3.26}$$

In this case the absolute values of arguments $z_{I,II}$ of the Fresnel integral are large within the whole domain of the t'-integration in (3.21-3.22) except the vicinity of the upper limit t. On the other hand, one can expect that in the internal region W the wave function at large times contains mainly the bound states (if there is no zero modes in the potential V). This is because the scattered wavepacket disperses over a large volume as t increases. Thus, the contribution from the vicinity of the upper limit t, in the integrals (3.21-3.22), is suppressed due to the smallness of the magnitude of μ and ν, determined by the values of the bound states at the boundaries $a_{\pm}$. In the rest of the integration domain, the asymptotic expansion for the Fresnel integral Φ can be used:

$$\Phi(z) = \begin{cases} 1 + \dfrac{\mathrm{e}^{\mathrm{i}\frac{\pi}{4}}}{2z\sqrt{\pi}}\mathrm{e}^{\mathrm{i}z^2} + O(z^{-3}), & z \to -\infty, \\ \dfrac{\mathrm{e}^{\mathrm{i}\frac{\pi}{4}}}{2z\sqrt{\pi}}\mathrm{e}^{\mathrm{i}z^2} + O(z^{-3}), & z \to +\infty. \end{cases} \tag{3.27}$$

One can neglect the terms of order $1/z$ in the expansion (3.27), provided that the following conditions are valid

$$Et \gg 1. \tag{3.28}$$

In the latter case, no contribution from $\widehat{\Psi}^{I,II}(-q,t)$ comes to the amplitude (3.19). Also, by virtue of orthogonality between the bound states ψ_n and the scattering states $\psi^{(-)}_{1,2E}$ the last integrals with respect to the region W in the expression (3.19) can be neglected.

As a result, the amplitudes in this approximation are determined by $\widehat{\Psi}^{I,II}(q,t)$ only and its final form via the probability flux in this approximation is

$$\mathcal{A}_{\pm qn} \simeq \pm\mathrm{e}^{\mathrm{i}\phi_{\pm}}\int_{t_0}^{t}\mathrm{d}t' j[\Psi(x,t'), \Theta_{\pm q + \frac{\tau}{c}A_-}(x,t')]\Big|_{x=a_{\pm}} \tag{3.29}$$

Here the values of the phases $\phi_{\pm}$ are not important for evaluation of the function $p_n(E)$, the flux j is

$$j[\Psi,\Phi] = \frac{\mathrm{i}}{2}\left\{\Psi D^*\Phi^* - \Phi^* D\Psi\right\}, \tag{3.30}$$

and $\Theta_k(x,t)$ is the Volkov function (2.20).

One can expect this expression to give a reasonably accurate approximation for not very small energies E or sufficiently large times t. The approximative equality in (3.29) becomes exact under simultaneous passing to limit $(t-t_0) \to +\infty$ and $|a_{\pm}| \to +\infty$.

IV. NUMERICAL METHOD

Now we formulate a numerical method which will be applied below to solving, on a time-space grid, a one-dimensional TDSE (1.1). For time-integration we shall use the Crank–Nicolson scheme that provides the accuracy of order $O(\tau^2)$ for each time-step τ. The operator form of this scheme is

$$\left(I + \frac{\mathrm{i}\tau}{2}H(t_{k+\frac{1}{2}})\right)\Psi^{k+1} = \left(I - \frac{\mathrm{i}\tau}{2}H(t_{k+\frac{1}{2}})\right)\Psi^{k}, \quad t_k = t_0 + k\tau, \tag{4.1}$$

where the solution $\Psi^k(x)$ discretized with respect to time corresponds to $\Psi(x,t_k)$ and depends only on the space variable $x \in \mathbb{R}$. This scheme will be implemented with the help of the Galerkin method [25]. In this way, a system of algebraic finite difference equations is obtained at each step k. In the internal region W, the solution Ψ^k is sought as an expansion on a set of basis functions $\eta_j(x)$,

$$\Psi^k(x) = \sum_j u_j^k \eta_j(x), \quad x \in W. \tag{4.2}$$

Making use of the Galerkin method one finds the following system of the equations.

$$\sum_j\left\{\hat{m}_{j'j} + \frac{\mathrm{i}\tau}{2}\hat{h}^{k+\frac{1}{2}}_{0j'j}\right\}u_j^{k+1} - \sum_j\left\{\hat{m}_{j'j} - \frac{\mathrm{i}\tau}{2}\hat{h}^{k+\frac{1}{2}}_{0j'j}\right\}u_j^{k} = \\ = \frac{\mathrm{i}\tau}{2}\eta_{j'}(a_+)\nu^{II}(t_{k+\frac{1}{2}}) - \frac{\mathrm{i}\tau}{2}\eta_{j'}(a_-)\nu^{I}(t_{k+\frac{1}{2}}). \tag{4.3}$$

Here $\hat{m}$ is the overlap matrix, $\hat{m}_{j'j} = (\eta_{j'},\eta_j)$.

The right-hand side is the flux terms from the boundaries arising as a result of integration by parts of the expression $(\eta_{j'}, H(t_{k+\frac{1}{2}})\eta_j)$ and $\hat{h}^{k+\frac{1}{2}}_{0j'j}$ is the Hermitian matrix

$$\hat{h}^{k+\frac{1}{2}}_{0j'j} = \int_{a_-}^{a_+}\mathrm{d}x\left\{\frac{1}{2}D^*_{k+\frac{1}{2}}\eta_{j'}D_{k+\frac{1}{2}}\eta_j + V\eta_{j'}\eta_j\right\}. \tag{4.4}$$

The time point $t_{k+\frac{1}{2}} = t_k + \frac{\tau}{2}$ is intermediate point between t_k and t_{k+1}.

Thus, a boundary conditions are required to express $\nu^{I,II}(t_{k+\frac{1}{2}}) \approx (\nu^{I,II}_{k+1} + \nu^{I,II}_k)/2$ via $\mu^{I,II}_k$ and $\mu^{I,II}_{k+1}$. In turn, let us consider the finite difference representation of the eq. (3.3) on the mesh grid t_k. The integrand contains the square root singularity at the end point t, so the quadrature rule chosen for the approximative representation of the integral over time should takes into account this singular point in order to obtain a reasonable accuracy. The following interpolating quadrature rule on the uniform knot sequence with the step τ was chosen:

$$\int_0^{k\tau} t^{-1/2} f(t)\mathrm{d}t \approx \sum_{s=0}^{k} a^{(k)}_s f(s\tau), \quad a^{(k)}_0 = \frac{4\tau^{1/2}}{3},$$
$$a^{(k)}_k = a^{(k)}_0\{(k-1)^{3/2} - (k-3/2)k^{1/2}\}, \quad a^{(k)}_s = a^{(k)}_0\{(s-1)^{3/2} - 2s^{3/2} + (s+1)^{3/2}\}. \tag{4.5}$$

With the help of this rule the finite difference representation of the boundary conditions takes the form

$$\nu^{I,II}_k = \pm\frac{(2\pi\mathrm{i})^{1/2}}{\mathrm{i}a^{(k)}_0}\mu^{I,II}_k + f^{I,II}_k, \tag{4.6}$$

and $f^{I,II}_k$ is

$$f^{I,II}_k = -\sum_{s=0}^{k-1}\left(\frac{a^{(k)}_{k-s}}{a^{(k)}_0}\right)\mathrm{e}^{\mathrm{i}S_{ks}}\left\{\nu^{I,II}_s - \mathrm{i}P_{ks}\mu^{I,II}_s\right\} \mp \frac{(2\pi\mathrm{i})^{1/2}}{\mathrm{i}a^{(k)}_0} 2F^{I,II}_{as}(t_k). \tag{4.7}$$

Here

$$S_{ks} = \frac{(\xi(t_k) - \xi(t_s))^2}{2(t_k - t_s)} - \frac{1}{2}\int_{t_s}^{t_k} A^2(t')\mathrm{d}t', \quad P_{ks} = \frac{\xi(t_k) - \xi(t_s)}{t_k - t_s} + A(t_s). \tag{4.8}$$

Some simplification in the (4.8) connected with dropping the $\frac{1}{2}\int A^2\mathrm{d}t'$ term can be achieved by the unitary transformation of the original TDSE (1.1) $\Psi \to \mathrm{e}^{\frac{\mathrm{i}}{2}\int_0^t A^2(t')\mathrm{d}t'}\Psi$.

Thus, using (4.6), (4.2) and (4.3) one finds the final form of the system of algebraic equations,

$$\left(\hat{m} + \frac{\mathrm{i}\tau}{2}\hat{h}^{k+\frac{1}{2}}\right)\mathbf{u}^{k+1} = \left(\hat{m} - \frac{\mathrm{i}\tau}{2}\hat{h}^{k+\frac{1}{2}}\right)\mathbf{u}^{k} + \frac{\mathrm{i}\tau}{2}\mathbf{d}^{k+\frac{1}{2}}, \tag{4.9}$$

where

$$\hat{h}^{k+\frac{1}{2}}_{j'j} = \hat{h}^{k+\frac{1}{2}}_{0j'j} + \frac{(2\pi\mathrm{i})^{1/2}}{2\mathrm{i}a^{(k)}_0}\left\{\eta_{j'}(a_-)\eta_j(a_-) + \eta_{j'}(a_+)\eta_j(a_+)\right\}, \tag{4.10}$$

and

$$(\mathbf{d}^{k+\frac{1}{2}})_j = \eta_j(a_+)\frac{f^{II}_k + f^{II}_{k+1}}{2} - \eta_j(a_-)\frac{f^{I}_k + f^{I}_{k+1}}{2}. \tag{4.11}$$

Below in all calculation we use the cubic B-splines [26] as a set of the basis functions $\eta_j(x)$. Such choice leads to systems of algebraic equations with band matrixes and its inversion can be effectively performed by Gauss elimination method.

V. NUMERICAL RESULTS AND DISCUSSION

A. Model

For an illustration of the method which uses the IBC, we now consider the solution of the time-dependent Schroedinger equation that describes a one-dimensional atom modeled by the Pöschl-Teller potential $V_{PT}(x)$ [27]. This potential was earlier used in [15] and our results allow a direct comparison to their work.

$$V_{PT}(x) = -\frac{1}{\cosh^2 x}, \quad |x| < \infty \tag{5.1}$$

Such potential supports only one bound state,

$$\psi_0(x) = \frac{1}{\sqrt{2}\cosh x}, \tag{5.2}$$

with eigenenergy $E_0 = -1/2$, and a continuum of the scattering states

$$\psi^{(+)}_{1,2E}(x) = \frac{\mathrm{i}q \mp \tanh x}{1 + \mathrm{i}q}\mathrm{e}^{\pm\mathrm{i}qx}. \tag{5.3}$$

It follows from eq. (5.3) that there is an additional, pseudobound state with $E = 0$. This states become a real bound state if one increases the depth of the potential well.

The vector-potential $A(t)$ generating the laser electric field $\mathcal{E}(t)$ was chosen in all calculations in the form of a square pulse,

$$A(t) = \begin{cases} -\dfrac{\mathcal{E}_0}{\omega}\sin\omega t, & 0 \le t \le T = \dfrac{2\pi N}{\omega}. \\ 0, & t < 0, \quad t > T, \end{cases} \tag{5.4}$$

where the duration of the pulse, T, is defined in terms of N periods of the laser angular frequency ω.

B. Wave packets

First, we consider the integration of the TDSE, eqs. (5.1)-(5.4), with the atom being initially in the ground state (5.2). In these calculations, two sets of the peak field parameter $\mathcal{E}_0$ were used for an 8-cycle pulse with $\omega = 0.1$: (*i*) $\mathcal{E}_0 = 0.1$, and (*ii*) $\mathcal{E}_0 = 0.2$, with the excursion amplitude of the electron ξ_0 being 10 and 20 au, respectively.

Integration with respect to time was carried out for the full duration of the pulse, $0 \le t \le T$.

In all calculations by the IBC method the boundaries of the internal region W were taken to be $a_\pm = 10$ au as shown in Fig. 1 (a) and the integral boundary conditions (3.3) were imposed at $a_\pm$. The numerical solution in W was obtained by using the Crank-Nicolson-Galerkin method described above. Because the initial state (5.2) falls off

exponentially, the terms $F_{as}^{I,II}$ in (3.3) at the boundaries are of order $\sim 10^{-5}$, and these terms were neglected. The potential V_{PT} vanishes even more rapidly, so that the solution could be accurately extended to the external regions I and II by using the asymptotic representation (3.15).

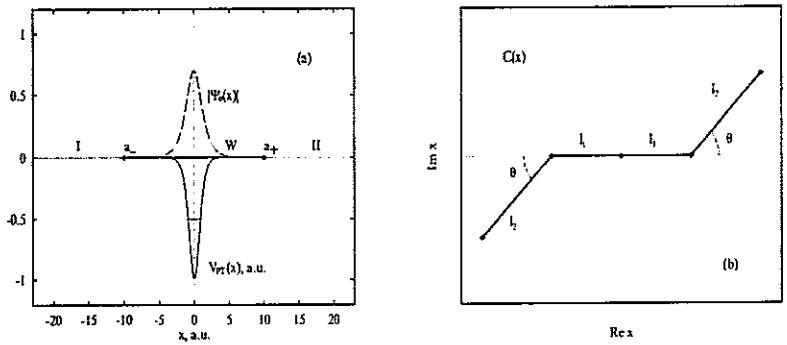

FIG. 1. (a) Division of space $\mathbb{R}$ into regions I, II and W for integration by the IBC method; the box size (region W) is ± 10 au; the initial ground state (supported by the Pöschl-Teller potential) has eigenenergy $E = -0.5$ au. (b) The contour $C(x)$ in the complex x-plane used in the CC calculations of the same problem.

For comparison, the same problem has also been solved numerically by the complex coordinate method (CC) and by imposing the rigid boundary conditions (1.2) at the outer edge of a very large space-grid.

For the CC method, the complex contour $C(x)$ is shown in Fig. 1 (b) where l_1 and l_2 specify the integration domain on the complex plane x. The principle moment of this method is that the complex parts of $C(x)$ provide exponential decay of the functions $e^{ikC(x)}$ for $x > l_1$ and $e^{-ikC(x)}$ for $x < -l_1$. The rate of this decay depends on the angle θ, $0 < \theta < \frac{\pi}{2}$.

Thus, the outgoing from the origin wave packets disappear as they propagate past $\pm l_1$ on the complex part of the contour $C(x)$. The reflection of the wave packets from rigid boundaries chosen sufficiently large is strongly suppressed in this case. The lengths l_2 should be chosen in such a way that the outgoing wavepackets on real axis not be appreciably scattered back towards origin by the action of the electric field and potential beyond $\pm l_1$. So that, at least, the two parameters, l_2 and θ, are need to select for using the CC method. Below we for definiteness assume $l_1 = l_2$, and the angle θ only considered as adjust parameter of the contour $C(x)$. For too small angles the reflection appears from the boundaries, but the choice of too large angles leads to collapse of the scheme because of the wavepackets returning back to small x grow exponentially on the complex parts of the contour $C(x)$.

The wave packets obtained at the end of the pulse ($t = T$) by the CC method as well as by the IBC method, are displayed in Figs. 2 (a, b). As shown below, the IBC results in these graphs are virtually exact.

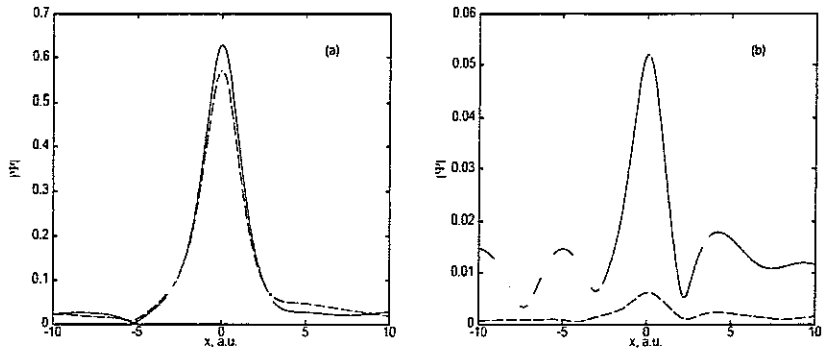

FIG. 2. Wave packet dynamics after application of a 8-cycle square laser pulse with $\omega = 0.1$ au. (a) $\mathcal{E}_0 = 0.1$ au; (b) the same with $\mathcal{E}_0 = 0.2$ au. Solid curve - solution obtained by the IBC method; broken curve - solution obtained by the CC method. For the IBC method, boundaries are at ± 10 au. For the CC method, the contour $C(x)$ has parameters $l_1 = l_2 = 10$ au. The best angle θ is 10^o in (a) and 5^o in (b).

In Figs. 2 (a, b), we use a contour $C(x)$ with $l_1 = l_2 = 10$ au so that the length of the real part of $C(x)$ is taken the same as in the IBC calculations. The angle θ is chosen to achieve the best possible agreement with the IBC solution on the interval $-10 \le x \le 10$. In Fig. 2 (a), agreement between the CC and IBC is moderate. However, there is a huge difference between the wave packets in Fig. 2 (b). This indicates that the chosen dimensions of $C(x)$ are too small. It follows, in fact, from our numerical experiments that for the field $\mathcal{E}_0 = 0.1$ au, l_1 should be taken at least 30 a.u., and for the field $\mathcal{E}_0 = 0.2$ au, at least 50 au. Thus, the size of the spatial grid which is required in the CC calculations is about ten times larger then the grid for the IBC method provided that we want to obtain a comparable accuracy of the numerical solutions.

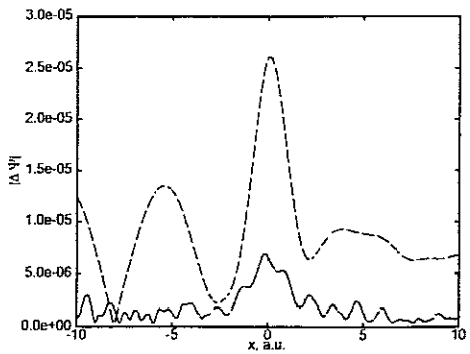

FIG. 3.Absolute difference between the solution obtained by the IBC method with $a_\pm = \pm 10$ au and the rigid-boundary solution which uses a very large space-grid ($a_\pm \approx \pm 1000$ au): (i) solid curve - for $\mathcal{E}_0 = 0.1$ au, and (i) broken curve - for $\mathcal{E}_0 = 0.2$ au. Integration steps: $\Delta x = 0.1$ au; $\tau = 5 \times 10^{-2}$ au for (i) and $\tau = 2.5 \times 10^{-2}$ au for (ii).

As our numerical experiments show, the numerical solution which used the rigid boundary conditions (1.2) needs spatial grids with the boundaries at least at $a_\pm = \pm 1000$ for the first set of field parameters, and $a_\pm = \pm 1500$ for the second set.

These large grids are consistent with earlier calculations by Eberly and co-workers [28] who used the reflective condition (1.2). For comparison between the solutions obtained by the IBC and full solutions with the boundary conditions (1.2) we explicitly calculate the absolute differences between both solutions (Fig. 3) as functions of x on interval W. It can be seen that the errors are of order 10^{-5}.

These results clearly demonstrate the superiority of the present IBC method. We point out that the increasing of the value ξ_0 leads to necessity to use larger size of the spatial grid, in contrast to the IBC method where the required size of the grid is determined by the decaying properties of the atomic potential only.

In the method of Boucke at al [15] where the Hamiltonian is assumed to be asymptotically field-free, one needs to use the Kramers-Henneberger frame, and the size of the grid also depends on the quiver ξ_0.

The IBC method allows also to take the scattering states (5.3) as initial state for TDSE to calculate free-free and free-bound transitions, in contrast to the CC method, where the incident plane wave contained in the scattering state exponentially grows on the contour $C(x)$. Similar comparisons for solutions obtained by IBC method and full solutions at large grid with proper logarithmic derivatives imposed at the boundaries show also the excellent agreement as far as for above bound initial state.

C. Energy distribution $p(E)$.

First, we consider the energy spectrum of photoelectrons ejected by the laser pulse. The computed energy distribution $p(E)$ for the electrons which are initially in the ground state (5.2), is shown in Fig. 4 for several values of $\mathcal{E}_0$.

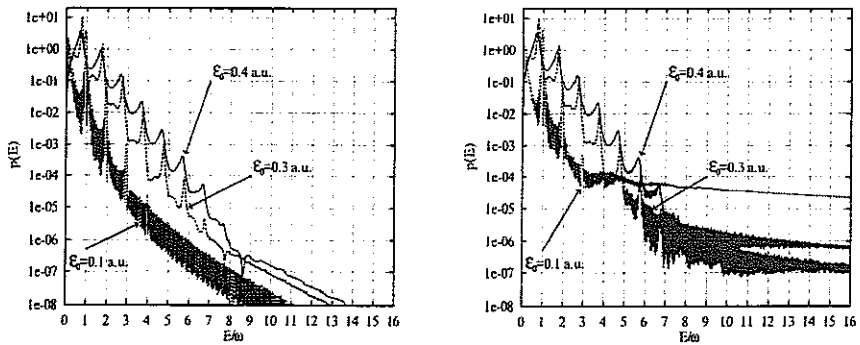

FIG. 4. The energy distribution $p(E)$ of laser-ejected electrons for several values of the field $\mathcal{E}_0$. A 16-cycle square laser pulse, with angular frequency $\omega = 0.5$ au. The function $p(E)$ is obtained using (a) the full expression (3.19) for amplitudes, and (b) the asymptotic expression (3.29). The pondermotive shifts of the ATI peaks are clearly seen.

The angular frequency ω of the field was chosen equal to the binding energy of the ground state $|E_0|$, $\omega = 0.5$ au.

Taking into account the pondermotive shift $U_p = \mathcal{E}_0^2/4\omega^2$, the position E_n of the peaks in the spectra is approximately given by $E_n = n\omega + E_0 - U_p$. This corresponds to absorbing by the electron the energy of n photons. For the laser parameters used in Figs. 4, the pondermotive shifts U_p which are 0.16, 0.09, and 0.01 au for $\mathcal{E}_0 = 0.4$, 0.3, and 0.1 au, respectively. These values give reasonable estimate of the exact numerical shifts obtained in present calculations.

The spectral distributions, shown in Figs. 4 (a, b) have been obtained in two different ways. In Fig. 4 (a), the spectral distributions $p(E)$ are calculated using the full amplitudes $\mathcal{A}_{\pm g0}$ (3.19-3.25). For $t = T$, this gives the exact result for $p(E)$. On the other hand, the distributions in Fig. 4 (b) have been obtained using the flux expression (3.29), with t taken up to T. The latter is valid only under condition (3.28). It can be seen from Fig. 4 that for the particular choice of laser parameters, the asymptotic expression (3.29) gives a good estimate for the energy distribution $p(E)$. The positions and heights of the ATI peaks are correctly reproduced. However, at the bottom of continuum, the asymptotic expression (3.29) cannot be applied and one needs to use the full expression (3.19).

As Figs. 4 show, the asymptotic formula for $p(E)$ works better for stronger fields $\mathcal{E}_0$. Qualitatively, this is because the electrons leave domain W faster when exposed to stronger fields. For a fixed value of T, this facilitates the condition (3.28.) We also point out that fast oscillations seen is some curves in Figs. 4 can be traced to the steep front of the pulse (5.4).

At small intensities of the field, the exact energy distributions $p(E)$ can be used for establishing the validity region of the standard perturbation theory. As an illustration, we consider transitions from the (even-parity) ground state $\psi_0(x)$ (5.2) to the (odd-parity) pseudobound state with energy $E = 0$.

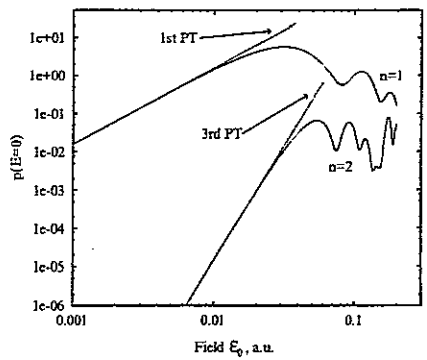

FIG. 5. Comparison between the exact calculations and perturbation theory. Probability density $p(E = 0)$ as a function of the laser field $\mathcal{E}_0$, for the electron transition from the ground state with $E_0 = -0.5$ au to a pseudobound state with $E = 0$. A 16-cycle laser pulse with angular frequency $\omega = 0.5$ au ($n = 1$) and 8-cycle pulse with $\omega = 0.25$ au ($n = 2$).

As the first example, we take $\omega = |E_0| = 0.5$ au. The leading term is one-photon

absorption, $n = 1$. In the lowest (1st) order of perturbation theory, $p(E)$ is generally given by

$$p^{(1)}(E) = \frac{1}{2\pi}\sum_{s=1}^{2}\left|\int_0^T \mathrm{d}t e^{i\Omega t}\langle\psi_{s,q}^{(-)}|\frac{e}{c}pA(t)|\psi_0\rangle\right|^2 = \frac{\pi\mathcal{E}_0^2\Omega}{\cosh^2\frac{\pi q}{2}}\frac{\sin^2\frac{(\Omega-\omega)}{2}T}{(\Omega^2-\omega^2)^2}, \qquad (5.5)$$

where $\Omega = E - E_0$. A comparison between both methods for the transition to the $E = 0$ level, is presented in Fig. 5 ('1st PT' and 'n=1' curves). As can be seen, in this case, perturbation theory works well up to $\mathcal{E}_0 \approx 0.01$ au.

As the second example, we take $\omega = 0.25$ au. The leading term is now two-photon absorption. It follows immediately from the parity consideration, that the 2nd order term $p^{(2)}(E = 0)$ vanishes, and the leading term of perturbation theory is $p^{(3)}(E = 0)$. In Fig. 5, the corresponding curves are marked '3rd PT' and 'n=2'. The validity region of perturbation theory extends, in this case, up to $\mathcal{E}_0 \approx 0.03$ au.

D. Ionization probability

For the comparison of our calculations with the calculations performed in [15], we evaluate the ionization probability of the atom, $w(\mathcal{E}_0) = 1 - p_{00}$, where the ground-state probability p_{00} is given, at the end of the square pulse, by (3.12). As in [15], we used 4- and 8-cycle pulses with the angular frequency $\omega = 0.2$ au.

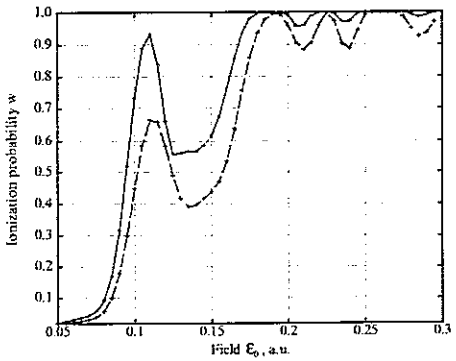

FIG. 6. Square laser pulse with angular frequency $\omega = 0.2$ au. Variation of the ionization probability w with the laser field $\mathcal{E}_0$ at the end of a 4-cycle (broken curve) and 8-cycle (solid curve) pulse.

The curves (see Fig. 6) produced in these calculations are identical with the ionization curves in Fig. 3 (a) of Ref. [15]. The ionization minima in the Fig. 6 are due to the effect of channel closing caused by the dynamical shift of the free-electron energy, U_p. By energy conservation, an n-photon channel is open only if $n\omega + E_0 > U_p$.

The threshold fields are $\mathcal{E}_0 = 0.126$, 0.219, and 0.283 au for closing $n = 3$, 4, and 5-photon channels. The minima positions in the calculated ionization probability are found

to be in good agreement with the above estimate for $n = 3$ and 5, but it is not as good for $n = 4$ where $\mathcal{E}_0$ passes through the critical value 0.22 au for the over-barrier ionization.

VI. CONCLUSIONS

We have developed by application of the general theory of the parabolic potentials a method which permits to impose the exact boundary conditions on an intermediate surface to be used in the numerical solution of the time-dependent Schrödinger equation. It allows to substantially reduce the size of the space domain where integration is carried out numerically. The method is based on considering an exterior part of the configuration space separated from the internal region by a surface σ that divides conventionally the space to the (external) domain of semiclassical motion of the particle and to the (internal) domain where it is required the quantum-mechanical description. The accurate asymptotic behavior of the solution is represented by a time-dependent Green's function for a free electron moving in the external (laser) electric field. This allows us to formulate integral boundary conditions on the surface σ in terms of asymptotic parabolic potentials. The long-range Coulomb potential can also be included into consideration and the boundary condition for the case of the spherical surface σ is presented. Numerical examples considered in the paper demonstrate the advantages of the present theory. The energy spectra and ionization probabilities have been obtained by this method for finite times and its form have been investigated in limit of infinitely large times. The applications of the method to more realistic systems like as Hydrogen atom in laser field will be subject of forthcoming publications.

This work is partly supported by Grant No. 95-0512 from RFBR-INTAS.

REFERENCES

[1] G. Floquet, Ann. Ec. Norm. **13** (2), 47 (1883); J. H. Shirley, Phys. Rev. B **138** 979 (1965); S. I. Chu, Adv. At. Mol. Phys. **21** 197 (1985).

[2] M. Pont, D. Proulx, and R. Shakeshaft, Phys. Rev. A **44**, 4486 (1991); R. M. Potvliege and R. Shakeshaft, Adv. At. Mol. Opt. Phys. Suppl. **1** 373 (1992); B. Piraux and R. Shakeshaft, Phys. Rev. A **49**, 3903 (1994)

[3] P. G. Burke, P. Franken and C. J. Joachain, J. Phys. B: At. Mol. Opt. Phys. **24**, 761 (1991); O. Latinne, N. J. Kylstra, M. Dörr, J. Purvis, M. Terao-Dunseath, C. J. Joachain, P. G. Burke and C. J. Noble, Phys. Rev. Lett. **74** 46 (1995).

[4] K. C. Kulander, Phys. Rev. A **35**, 445 (1987); K. C. Kulander, K. J. Schafer and J. L. Krause, Phys. Rev. Lett. **66**, 301 (1991).

[5] K. C. Kulander, K. J. Schafer and J. L. Krause, Adv. At. Mol. Opt. Phys. Suppl. **1**, 247 (1992).

[6] O. Latinne, C. J. Joachain and M. Dörr, Europhys. Lett. **26** 333 (1994).

[7] A. Scrinzi and B. Piraux, Phys. Rev. A **58**, 1310 (1998).

[8] A. Goldberg and B. W. Shore, J. Phys. B **11**, 3339 (1978); C. Leforestier and R. E.Wyatt, J. Chem. Phys. **78**, 2334 (1983); R. Kosloff and D. Kosloff, J. Comput. Phys. **63**, 363 (1986); D. Neuhauser and M. Baer, J. Chem. Phys. **90**, 4351 (1989).

[9] J. L. Krause, K. J. Schafer and K. C. Kulander, Phys. Rev. A. **45** 4998 (1992).

[10] C. W. McCurdy and C. K. Stroud, Comput. Phys. Commun., **63** 323 (1991).

[11] Discussion of the size of the configuration space required for studying various laser-induced processes can be found for instance in Ref. [5].

[12] P. G. Burke and K. A. Berrington, Atomic and Molecular Processes: an R-matrix approach, IOP Publications, Bristol (1993).

[13] H. W. Jang and J. C. Light, J. Chem. Phys., **99** (2) 1057 (1993).

[14] P. G. Burke and V. Burke, J. Phys. B, **30** L383 (1997).

[15] K. Boucke, H. Schmitz and H.-J. Kull, Phys. Rev. **A56** 763 (1997).

[16] H. A. Kramers, Collected Scientific Papers (North-Holland, Amsterdam, 1956); W. C. Henneberger, Phys. Rev. Lett. **21** 838 (1968); H. L. Cycon, R. G. Froese, W. Kirsch, and B. Simon, Schrödinger operators with Applications to Quantum Mechanics and Global Geometry, Springer-Verlag, N.Y., 1987.

[17] S. G. Mikhlin, Linear equations of mathematical physics, Holt, Rinehardt and Winston, N.Y. (1967), and references therein.

[18] V. P. Maslov, Asymptotic methods and perturbation theory, Moscow, "Nauka", 1988, in Russian.

[19] M. C. Gutzwiller, Chaos in classical and quantum mechanics, Springer-Verlag, N.Y. (1991)

[20] Ref. [17], particularly, Ch. 6 by P. M. Riz and L. N. Slobodetsky.

[21] R. P. Feynman, Rev. Mod. Phys. **20** 367 (1948); A. I. Baz, Ya. B. Zeldovich, A. M .Perelomov, Scattering, reactions and decays in non-relativistic quantum mechanics, (in Russian), M., "Nauka", 1971, Ch V.

[22] L. D. Faddeev, S. P. Mercuriev, Quantum scattering theory for few-body systems, Moscow, "Nauka", 1985.

[23] L. D. Landau and E. M. Lifshitz, Quantum Mechanics (non-relativistic theory), Pegramon Press, Oxford (1975).

[24] A. M. Perelomov, V. S. Popov, and M. V. Terentiev, ZETP, **50** 1393 (1966); S. Geltman, J. Phys. B, **10** 831 (1977).

[25] V. A. Trenogin, Functional analysis (in Russian) Moscow, "Nauka", 1980, p. 331.

[26] C. de Boor, A Practical Guide to Splines N.Y., Springer-Verlag, (1978), p. 108.

[27] G. Pöschl and E. Teller, Z. Physik, **83** 143 (1933).

[28] J. Javanainen, J. H. Eberly, and Q. Su, Phys. Rev. A **38** 3430 (1988).

Received by Publishing Department
on May 28, 1999.